Supporting Information for

Responsive Ruthenium Complex Probe for Phosphorescence and Time-Gated Luminescence Detection of Bisulfite

Wenzhu Zhang,[a] Xiuyan Xi,[a] Yong-Lei Wang,[b] Zhongbo Du,[a] Chaolong Liu,[a] Jianping Liu,[b] Bo Song,[a] Jingli Yuan,[a]* and Run Zhang[c]**

[a] State Key Laboratory of Fine Chemicals, School of Chemical Engineering, Dalian University of Technology, Dalian 116024, China

[b] Department of Materials and Environmental Chemistry, Stockholm University, Stockholm, 10691, Sweden

[c] Australian Institute for Bioengineering and Nanotechnology, The University of Queensland, St. Lucia, QLD 4072, Australia

Table of Contents

1. General information

Reagents and instruments

4-Bromo-1,10-phenanthroline[1] and *cis*-$Ru(bpy)_2Cl_2 \cdot 2H_2O$[2-3] were synthesized following literature methods. 2,4-Dinitroaniline and phenol were purchased from Aladdin (China). Wine sample was purchased from local supermarket in Dalian, China. Unless otherwise stated, all the reagents used in experiments were obtained from commercial sources. The solvents and reagents are analytical grade from commercial suppliers, and were used directly without further purification. Deionized water was used throughout.

^1H NMR and ^{13}C NMR spectra were acquired on a Bruker Avance NMR spectrometer (500 MHz for ^1H and 100 MHz for ^{13}C). Mass spectra of the compounds were determined on a LTQ Orbitrap XL mass spectrometer and an Agilent 6224 mass spectrometer. Elemental analysis was performed on a Vario-EL analyser. UV-visible absorption spectra were recorded on a Perkin-Elmer Lambda 35 UV-vis spectrometer (1.0 cm quartz cell) at 25 ^oC. Phosphorescence (0 ns delay time) and time-gated luminescence (TGL, 100 ns delay time) spectra were recorded using an Edinburgh FS5 spectrometer with excitation and emission slits of 3 nm (1.0 cm quartz cell) at 25 ^oC.

Theoretical calculation

The theoretical computation was conducted by using the Gaussian 09 package of programs.[4] The molecular structures of **Ru-azo** and **Ru-SO3** at ground-states and excited states were firstly optimized using the density functional theory (DFT).[5] Based on these optimized molecular structures, the related excited-state calculations were then conducted by the time-dependent DFT (TD-DFT) method. The Beck's three-parameter hybrid functional with the Lee-Yang-Parr correlation functional (B3LYP)[6] was used throughout. The LanL2DZ basis set[7] was used for Ru atoms in both complexes, whereas 6-311*G(d, p) basis set[8] was applied to hydrogen, carbon, nitrogen, sulphur and oxygen atoms. The polarized continuum model (PCM)[9] was employed for the solvent effects (water) in optimization, absorbance and emission calculations.

2. Synthesis and characterization of Ru(II) complexes

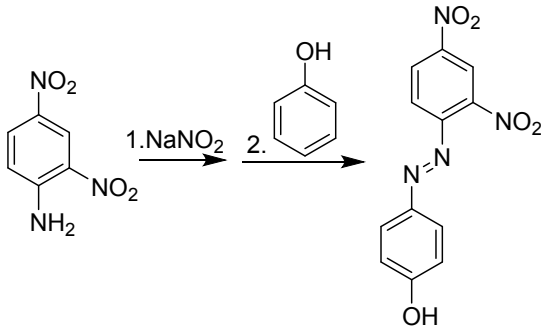

4-((2,4-dinitrophenyl)diazenyl)phenol

Scheme S1. Reaction pathway for the synthesis of 4-((2,4-dinitrophenyl)diazenyl)phenol.

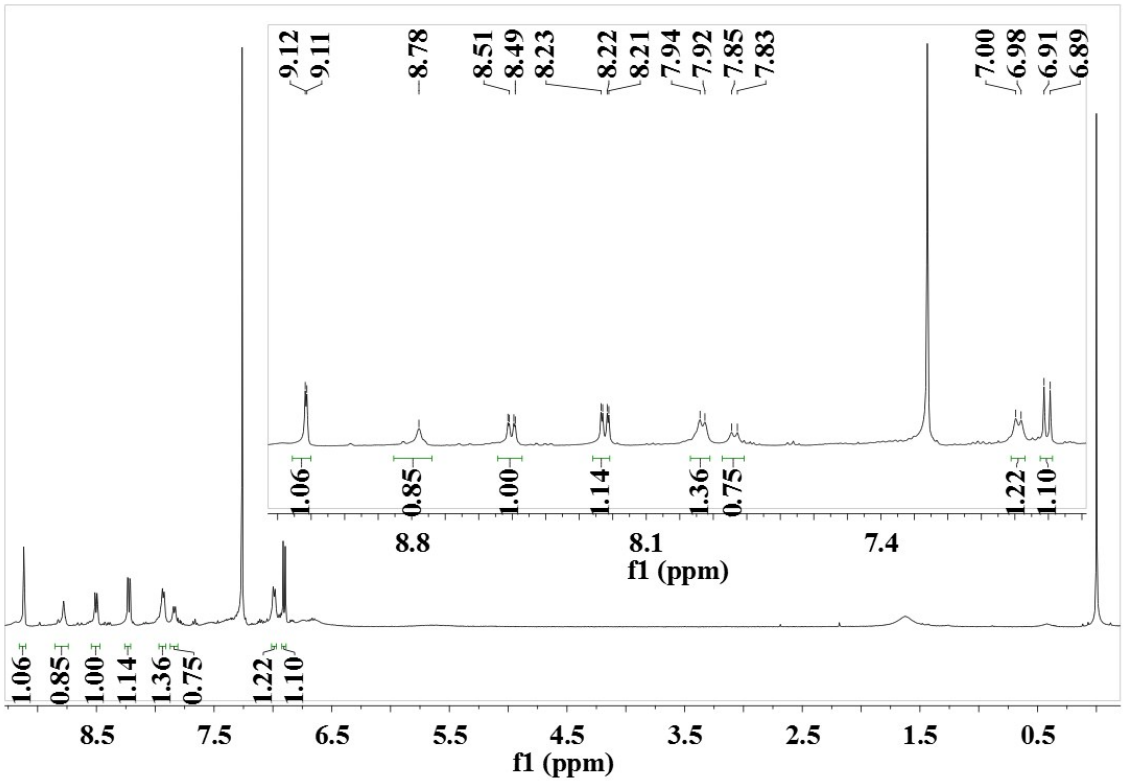

Fig. S1. ^{1}H NMR spectrum of 4-((2,4-dinitrophenyl)diazenyl)phenol in $CDCl_3$.

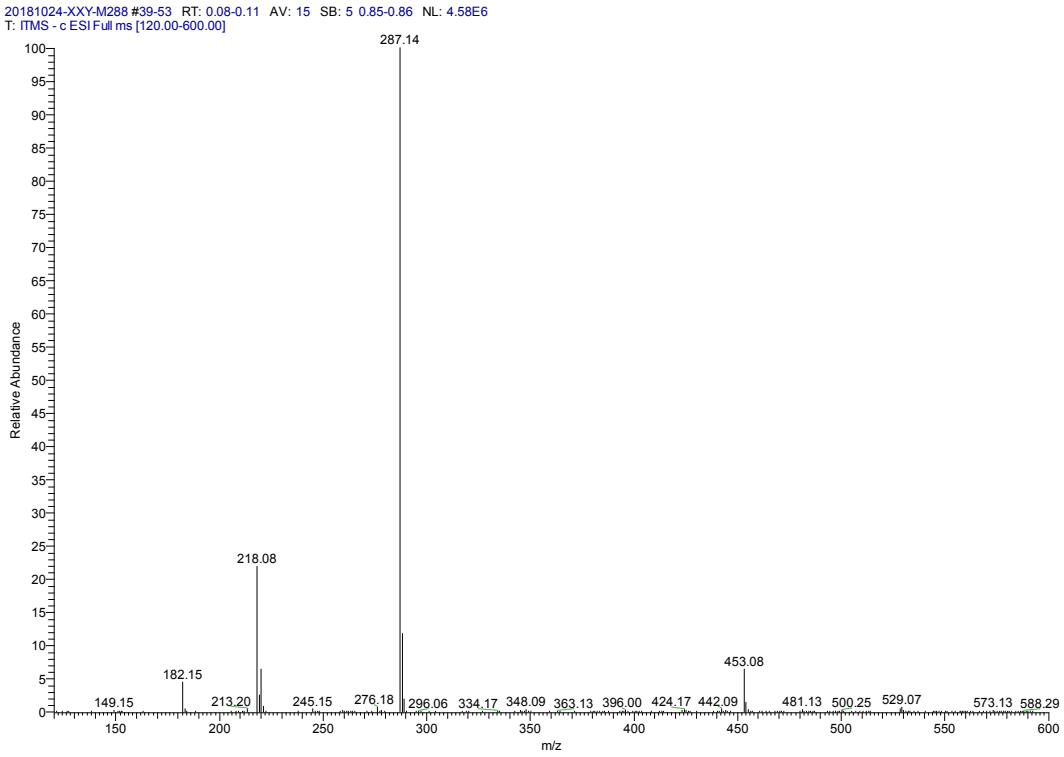

Fig. S2. ESI-MS of 4-((2,4-dinitrophenyl)diazenyl)phenol in $CHCl_3$.

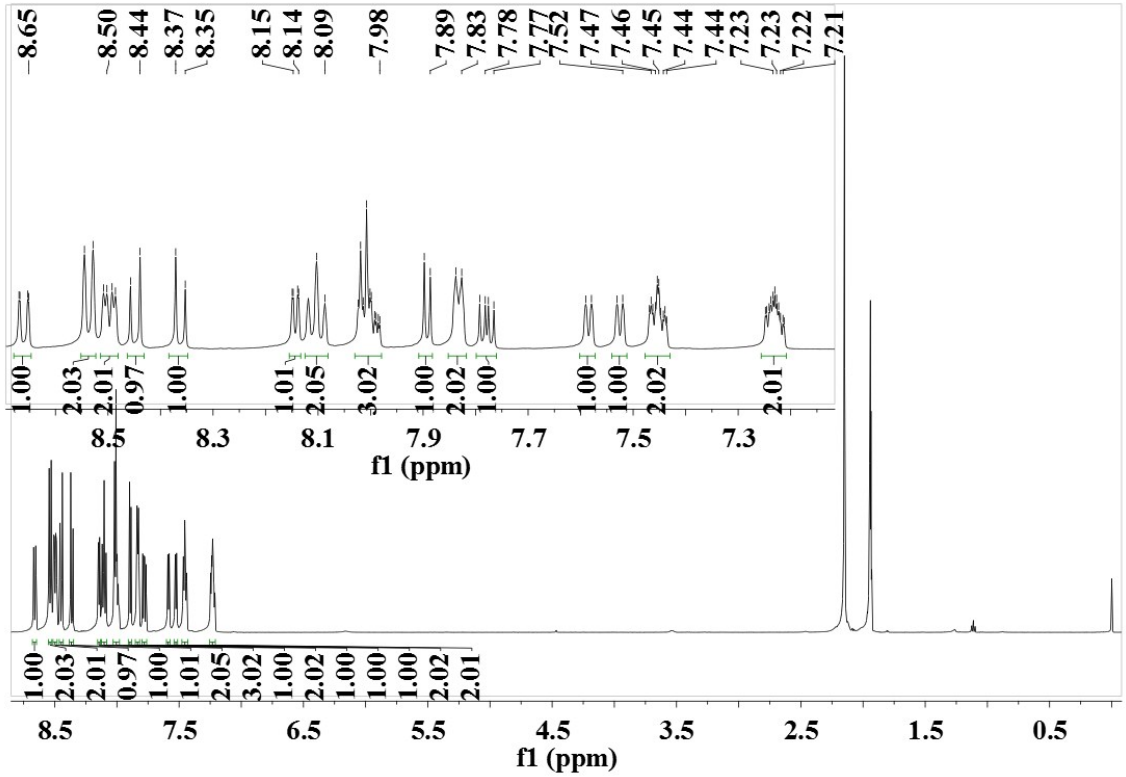

Fig. S3. ^{1}H NMR spectrum of $[Ru(bpy)_2(Br\text{-}phen)](PF_6)_2$ in CD_3CN.

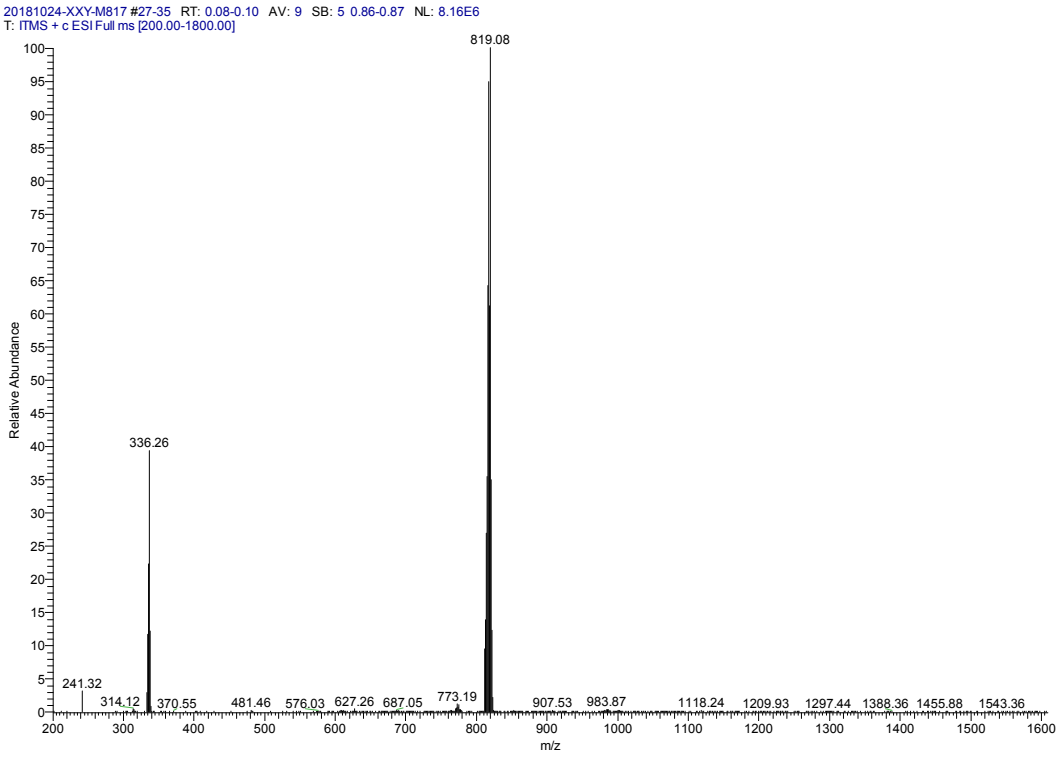

Fig. S4. ESI-MS of $[Ru(bpy)_2(Br\text{-}phen)](PF_6)_2$ in CH_3CN.

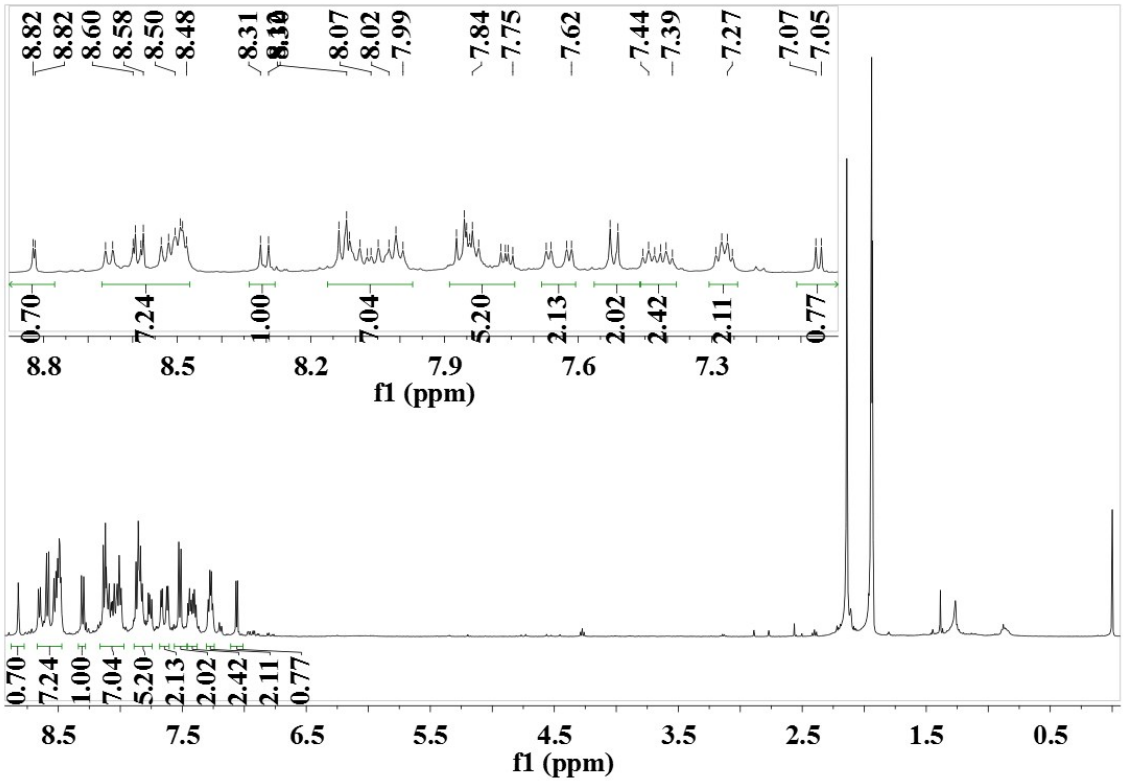

Fig. S5. ^1H NMR spectrum of **Ru-azo** in CD_3CN.

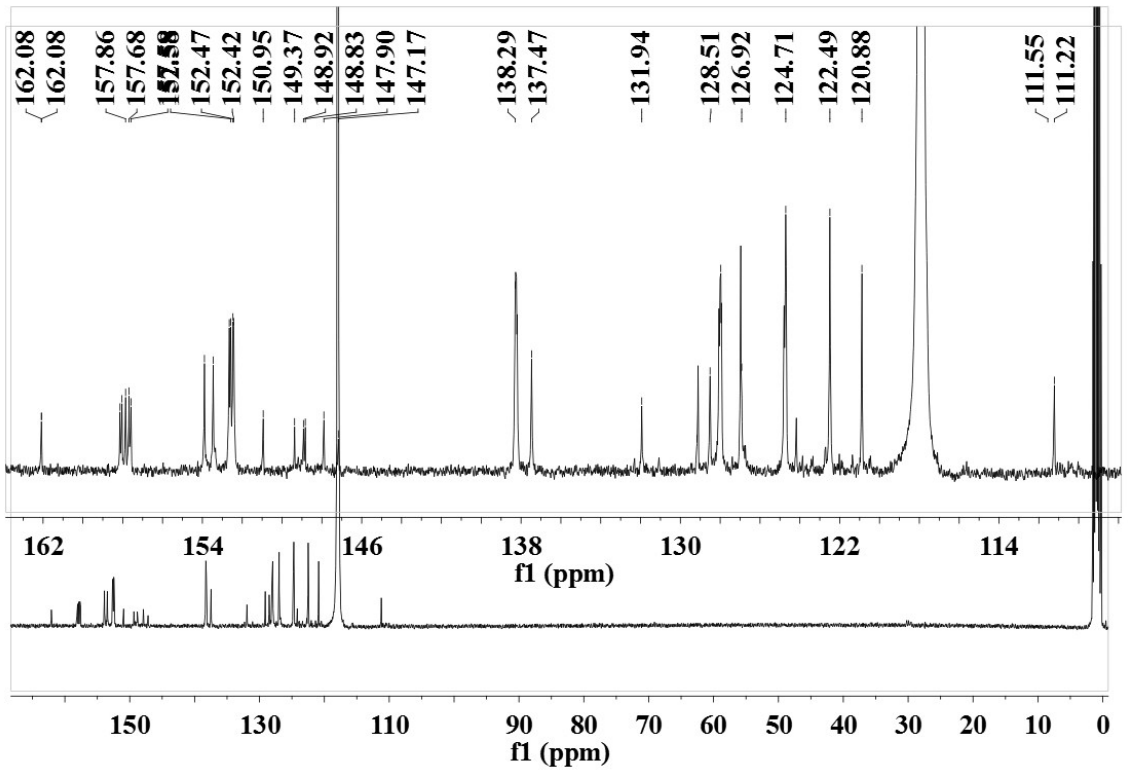

Fig. S6. ^{13}C NMR spectrum of **Ru-azo** in CD_3CN.

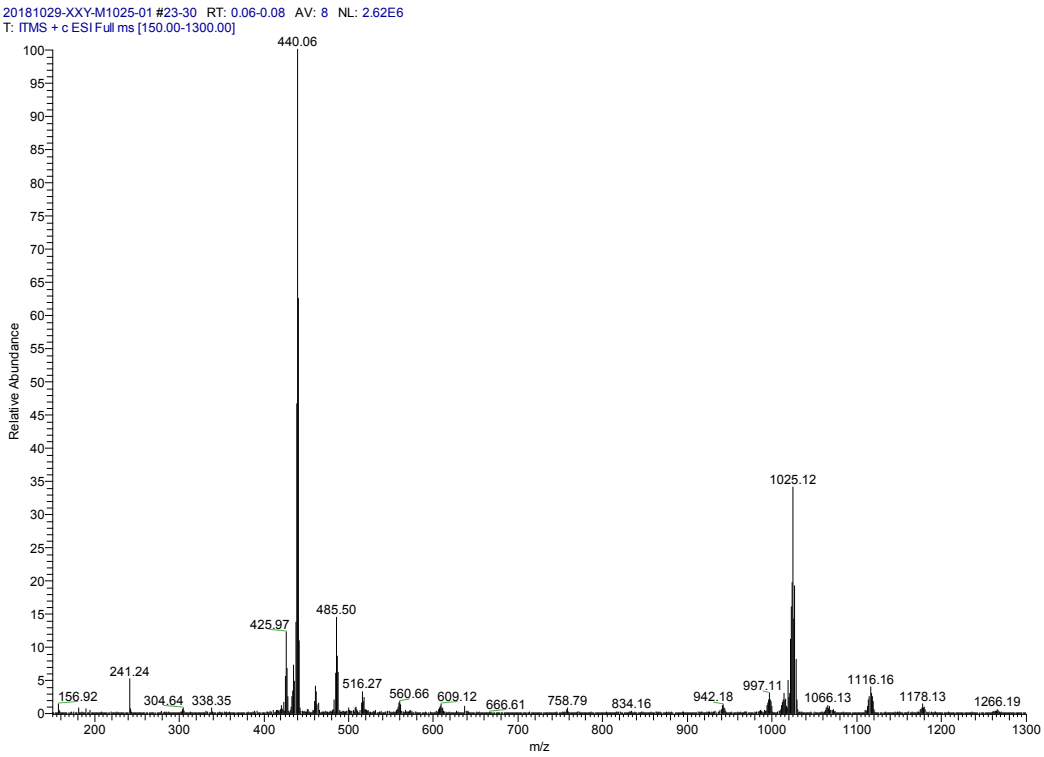

Fig. S7. ESI-MS of **Ru-azo** in CH_3CN.

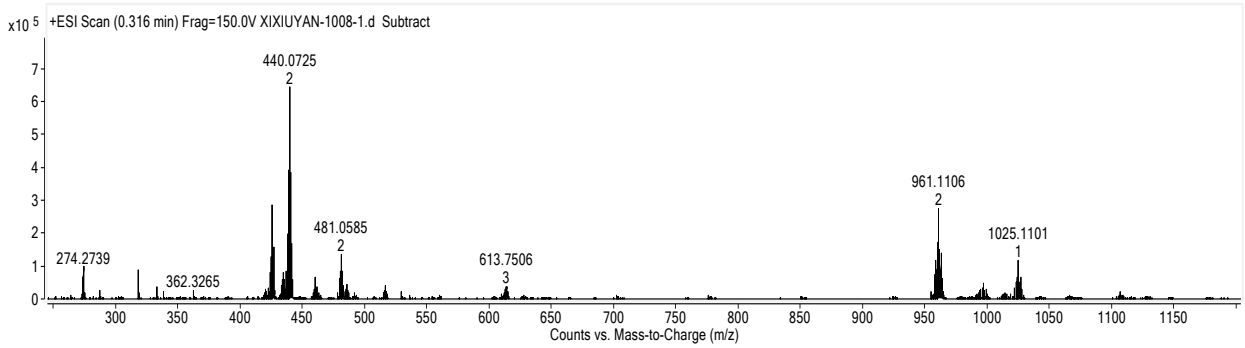

Fig. S8. HRMS of **Ru-azo** in the presence of bisulfite.

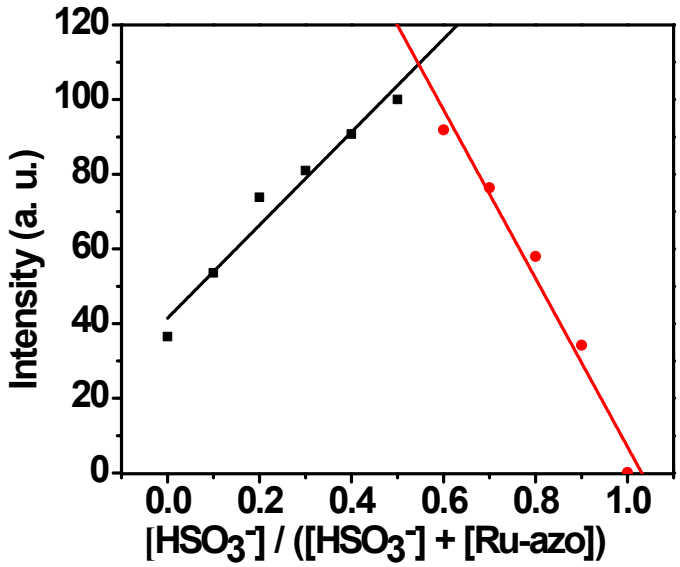

Fig. S9. Job plot analysis of the reaction between **Ru-azo** and HSO_3^- in PBS (25 mM, pH = 7.4). Total concentration of **Ru-azo** and HSO_3^- was at a constant at 10 μM. (λ_{ex} = 466 nm, λ_{em} = 635 nm).

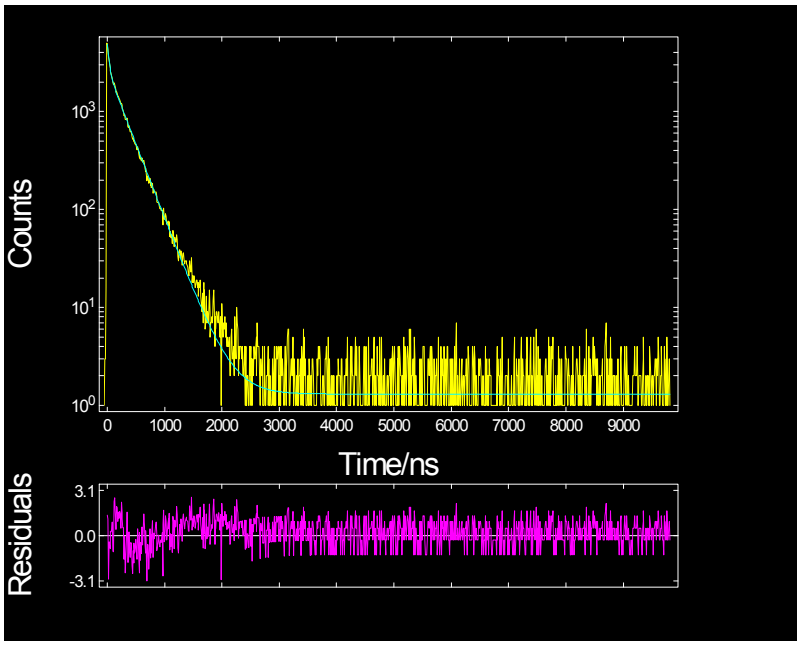

Fig. S10. Emission decay trace of **Ru-azo** in 25 mM PBS buffer of pH 7.4.

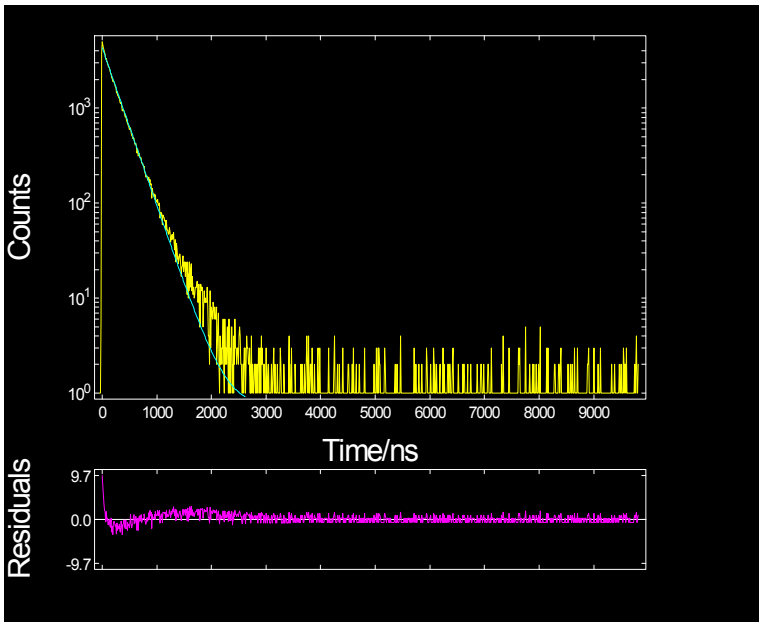

Fig. S11. Emission decay trace of **Ru-SO3** in 25 mM PBS buffer of pH 7.4.

3. Theoretical computations

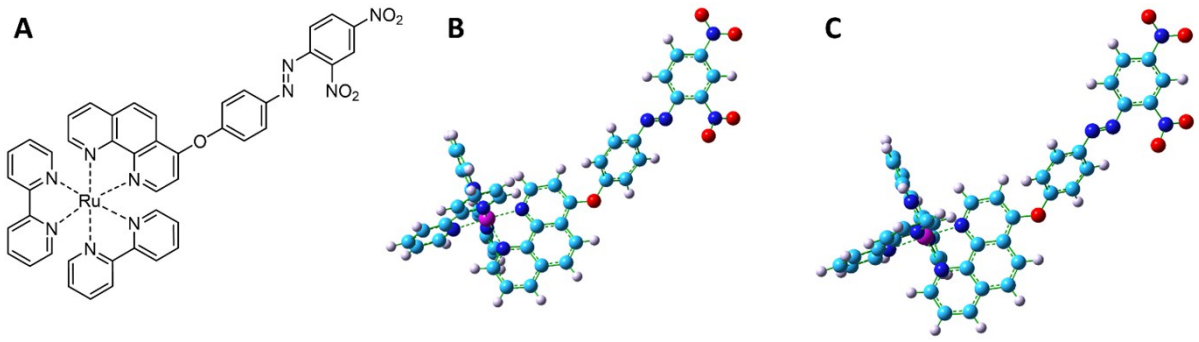

Fig. S12. Molecular structure of **Ru-azo** (A) and optimized molecular geometries of **Ru-azo** in the ground state (S_0) (B) and first triplet state (T_1) (C) obtained from DFT calculations at B3LYP//6-311+G(d, p)//LANL2DZ level of theory.

Table S1. Cartesian coordinates of **Ru-azo** in the ground state (S_0) and excited state (T_1).

Number	Atom	Coordinates (ground state S_0)			Coordinates (excited state T_1)		
		X	Y	Z	X	Y	Z
1	C	-3.8061	-2.5838	1.8196	-3.8061	-2.5838	1.8196
2	C	-3.6017	-3.6017	-0.4407	-3.6017	-3.2417	-0.4407
3	C	-3.3923	-4.5776	-0.0756	-3.3923	-4.5776	-0.0756
4	C	-3.3939	-4.9188	1.2897	-3.3939	-4.9188	1.2897
5	C	-3.6027	-3.9100	2.2425	-3.6027	-3.9100	2.2425
6	C	-4.0334	-1.4521	2.7398	-4.0334	-1.4521	2.7398
7	C	-4.4701	0.8644	2.9019	-4.4701	0.8644	2.9019
8	C	-4.4867	0.8053	4.3011	-4.4867	0.8053	4.3011
9	C	-4.2645	-0.4324	4.9330	-4.2645	-0.4324	4.9330
10	C	-4.0365	-1.5689	4.1419	-4.0365	-1.5689	4.1419
11	H	-3.6040	-2.9407	-1.4798	-3.6040	-2.9407	-1.4798
12	H	-3.2342	-5.3241	-0.8458	-3.2342	-5.3241	-0.8458
13	H	-3.6072	-4.1573	3.2969	-3.6072	-4.1573	3.2969
14	H	-4.6398	1.7967	2.3800	-4.6398	1.7967	2.3800
15	H	-4.6681	1.7085	4.8728	-4.6681	1.7085	4.8728
16	H	-3.8626	-2.5281	4.6140	-3.8626	-2.5281	4.6140
17	C	-1.9660	1.7176	0.0481	-1.9660	1.7176	0.0481
18	C	-0.6967	2.3471	0.1183	-0.6967	2.3471	0.1183
19	C	0.2501	0.1248	0.4924	0.2501	0.1248	0.4924
20	C	-1.0516	-0.4103	0.4031	-1.0516	-0.4103	0.4031
21	C	-3.1420	2.5064	-0.1780	-3.1420	2.5064	-0.1780
22	C	-3.0412	3.9140	-0.3433	-3.0412	3.9140	-0.3433
23	C	-4.2439	4.6406	-0.5702	-4.2439	4.6406	-0.5702
24	C	-5.4546	3.9512	-0.6197	-5.4546	3.9512	-0.6197
25	C	-5.4739	2.5464	-0.4429	-5.4739	2.5464	-0.4429
26	H	1.0800	-0.5438	0.6842	1.0800	-0.5438	0.6842
27	H	-1.2073	-1.4756	0.5123	-1.2073	-1.4756	0.5123
28	H	-6.3911	4.4699	-0.7907	-6.3911	4.4699	-0.7907
29	H	-6.4071	1.9988	-0.4725	-6.4071	1.9988	-0.4725
30	C	-5.4301	-0.7614	-2.5844	-5.4301	-0.7614	-2.5844
31	C	-3.1282	-0.3120	-2.8730	-3.1282	-0.3120	-2.8730
32	C	-3.2331	-0.4508	-4.2628	-3.2331	-0.4508	-4.2628
33	C	-4.4876	-0.7549	-4.8239	-4.4876	-0.7549	-4.8239
34	C	-5.5931	-0.9108	-3.9737	-5.5931	-0.9108	-3.9737
35	C	-6.5270	-0.9047	-1.6068	-6.5270	-0.9047	-1.6068
36	C	-7.1216	-0.7995	0.6778	-7.1216	-0.7995	0.6778
37	C	-8.4527	-1.1249	0.3887	-8.4527	-1.1249	0.3887
38	C	-8.8239	-1.3484	-0.9503	-8.8239	-1.3484	-0.9503
39	C	-7.8496	-1.2360	-1.9540	-7.8496	-1.2360	-1.9540
40	H	-2.1801	-0.0829	-2.4048	-2.1801	-0.0829	-2.4048
41	H	-2.3521	-0.3223	-4.8814	-2.3521	-0.3223	-4.8814
42	H	-6.7987	-0.6176	1.6943	-6.7987	-0.6176	1.6943

43	H	-9.1726	-1.2001	1.1959	-9.1726	-1.2001	1.1959
44	N	-3.8043	-2.2602	0.4802	-3.8043	-2.2602	0.4802
45	N	-2.1424	0.3529	0.1819	-2.1424	0.3529	0.1819
46	N	-6.1737	-0.6896	-0.2927	-6.1737	-0.6896	-0.2927
47	N	-4.1977	-0.4635	-2.0447	-4.1977	-0.4635	-2.0447
48	N	-4.2491	-0.2352	2.1310	-4.2491	-0.2352	2.1310
49	N	-4.3494	1.8333	-0.2238	-4.3494	1.8333	-0.2238
50	Ru	-4.1566	-0.2467	0.0381	-4.1566	-0.2467	0.0381
51	H	-8.1202	-1.4055	-2.9890	-8.1202	-1.4055	-2.9890
52	H	-6.5647	-1.1446	-4.3911	-6.5647	-1.1446	-4.3911
53	H	-4.6025	-0.8681	-5.8967	-4.6025	-0.8681	-5.8967
54	H	-9.8466	-1.6036	-1.2074	-9.8466	-1.6036	-1.2074
55	H	-3.2364	-5.9448	1.6054	-3.2364	-5.9448	1.6054
56	H	-4.2686	-0.5114	6.0151	-4.2686	-0.5114	6.0151
57	C	2.8974	1.5355	0.2263	2.8974	1.5355	0.2263
58	C	3.9511	1.9170	1.0821	3.9511	1.9170	1.0821
59	C	3.1043	0.6854	-0.8761	3.1043	0.6854	-0.8761
60	C	5.2379	1.4317	0.8410	5.2379	1.4317	0.8410
61	H	3.7444	2.5837	1.9125	3.7444	2.5837	1.9125
62	C	4.3972	0.1999	-1.1119	4.3972	0.1999	-1.1119
63	H	2.2904	0.4225	-1.5429	2.2904	0.4225	-1.5429
64	C	5.4658	0.5646	-0.2600	5.4658	0.5646	-0.2600
65	H	6.0645	1.7110	1.4850	6.0645	1.7110	1.4850
66	H	4.5970	-0.4525	-1.9562	4.5970	-0.4525	-1.9562
67	H	-4.2102	5.7179	-0.7011	-4.2102	5.7179	-0.7011
68	C	-1.7376	4.5295	-0.2728	-1.7376	4.5295	-0.2728
69	C	-0.6067	3.7764	-0.0477	-0.6067	3.7764	-0.0477
70	H	-1.6644	5.6055	-0.4014	-1.6644	5.6055	-0.4014
71	H	0.3707	4.2421	0.0051	0.3707	4.2421	0.0051
72	C	0.4303	1.5017	0.3460	0.4303	1.5017	0.3460
73	O	1.6526	2.1488	0.4809	1.6526	2.1488	0.4809
74	N	6.7291	0.0140	-0.6066	6.7291	0.0140	-0.6066
75	N	7.7233	0.3674	0.1347	7.7233	0.3674	0.1347
76	C	8.9551	-0.2759	-0.1467	8.9551	-0.2759	-0.1467
77	C	10.1774	0.3913	0.1393	10.1774	0.3913	0.1393
78	C	9.0179	-1.6290	-0.5585	9.0179	-1.6290	-0.5585
79	C	11.4140	-0.2542	0.0468	11.4140	-0.2542	0.0468
80	C	10.2423	-2.2881	-0.6827	10.2423	-2.2881	-0.6827
81	H	8.0887	-2.1512	-0.7577	8.0887	-2.1512	-0.7577
82	C	11.4266	-1.5911	-0.3707	11.4266	-1.5911	-0.3707
83	H	12.3340	0.2700	0.2736	12.3340	0.2700	0.2736
84	H	10.2906	-3.3210	-1.0067	10.2906	-3.3210	-1.0067
85	N	10.1923	1.8093	0.5186	10.1923	1.8093	0.5186
86	N	12.7175	-2.2793	-0.4865	12.7175	-2.2793	-0.4865
87	O	9.2747	2.5777	0.0704	9.2747	2.5777	0.0704

88	O	11.1454	2.2190	1.2732	11.1454	2.2190	1.2732
89	O	12.7228	-3.5036	-0.8614	12.7228	-3.5036	-0.8614
90	O	13.7854	-1.6289	-0.2080	13.7854	-1.6289	-0.2080

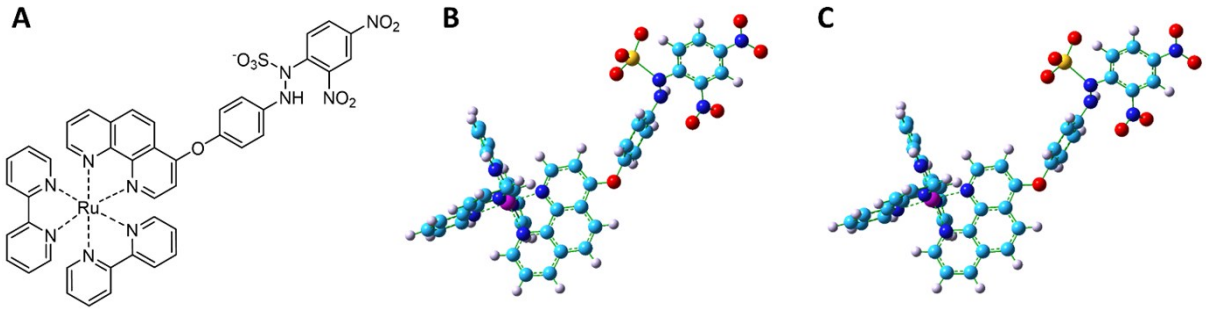

Fig. S13. Molecular structure of **Ru-SO3** (A) and optimized molecular geometries of **Ru-SO3** in the ground state (S_0) (B) and first triplet state (T_1) (C) obtained from DFT calculations at B3LYP//6-311+G(d, p)//LANL2DZ level of theory.

Table S2. Cartesian coordinates of **Ru-SO3** in the ground state (S_0) and excited state (T_1).

Number	**Atom**	**Coordinates (ground state S_0)**			**Coordinates (excited state T_1)**		
		X	Y	Z	X	Y	Z
1	C	4.1580	-2.4903	-1.7055	4.1580	-2.4903	-1.7055
2	C	3.8948	-3.1080	0.5601	3.8948	-3.1080	0.5601
3	C	3.6468	-4.4413	0.2105	3.6468	-4.4413	0.2105
4	C	3.6576	-4.8021	-1.1498	3.6576	-4.8021	-1.1498
5	C	3.9157	-3.8148	-2.1130	3.9157	-3.8148	-2.1130
6	C	4.4396	-1.3807	-2.6374	4.4396	-1.3807	-2.6374
7	C	4.9474	0.9193	-2.8245	4.9474	0.9193	-2.8245
8	C	4.9890	0.8386	-4.2221	4.9890	0.8386	-4.2221
9	C	4.7440	-0.4019	-4.8402	4.7440	-0.4019	-4.8402
10	C	4.4674	-1.5190	-4.0373	4.4674	-1.5190	-4.0373
11	H	3.8901	-2.7918	1.5948	3.8901	-2.7918	1.5948
12	H	3.4514	-5.1709	0.9883	3.4514	-5.1709	0.9883
13	H	3.9276	-4.0772	-3.1637	3.9276	-4.0772	-3.1637
14	H	5.1335	1.8546	-2.3134	5.1335	1.8546	-2.3134
15	H	5.2066	1.7276	-4.8032	5.2066	1.7276	-4.8032
16	H	4.2754	-2.4799	-4.4988	4.2754	-2.4799	-4.4988
17	C	2.4170	1.8906	-0.0375	2.4170	1.8906	-0.0375
18	C	1.1711	2.5579	-0.1455	1.1711	2.5579	-0.1455
19	C	0.1603	0.3598	-0.4942	0.1603	0.3598	-0.4942
20	C	1.4426	-0.2128	-0.3715	1.4426	-0.2128	-0.3715
21	C	3.6125	2.6471	0.1986	3.6125	2.6471	0.1986
22	C	3.5529	4.0605	0.3367	3.5529	4.0605	0.3367
23	C	4.7734	4.7530	0.5766	4.7734	4.7530	0.5766

24	C	5.9608	4.0277	0.6630	5.9608	4.0277	0.6630
25	C	5.9395	2.6202	0.5099	5.9395	2.6202	0.5099
26	H	-0.6904	-0.2853	-0.6734	-0.6904	-0.2853	-0.6734
27	H	1.5659	-1.2852	-0.4524	1.5659	-1.2852	-0.4524
28	H	6.9094	4.5202	0.8445	6.9094	4.5202	0.8445
29	H	6.8541	2.0439	0.5670	6.8541	2.0439	0.5670
30	C	5.7517	-0.6384	2.7062	5.7517	-0.6384	2.7062
31	C	3.4573	-0.1210	2.9349	3.4573	-0.1210	2.9349
32	C	3.5292	-0.2308	4.3293	3.5292	-0.2308	4.3293
33	C	4.7633	-0.5541	4.9241	4.7633	-0.5541	4.9241
34	C	5.8819	-0.7593	4.1018	5.8819	-0.7593	4.1018
35	C	6.8634	-0.8352	1.7550	6.8634	-0.8352	1.7550
36	C	7.5080	-0.7956	-0.5182	7.5080	-0.7956	-0.5182
37	C	8.8215	-1.1580	-0.1946	8.8215	-1.1580	-0.1946
38	C	9.1575	-1.3668	1.1562	9.1575	-1.3668	1.1562
39	C	8.1669	-1.2027	2.1365	8.1669	-1.2027	2.1365
40	H	2.5266	0.1220	2.4398	2.5266	0.1220	2.4398
41	H	2.6391	-0.0654	4.9258	2.6391	-0.0654	4.9258
42	H	7.2123	-0.6242	-1.5449	7.2123	-0.6242	-1.5449
43	H	9.5551	-1.2728	-0.9847	9.5551	-1.2728	-0.9847
44	N	4.1446	-2.1471	-0.3710	4.1446	-2.1471	-0.3710
45	N	2.5540	0.5186	-0.1448	2.5540	0.5186	-0.1448
46	N	6.5440	-0.6358	0.4295	6.5440	-0.6358	0.4295
47	N	4.5398	-0.3190	2.1339	4.5398	-0.3190	2.1339
48	N	4.6806	-0.1619	-2.0419	4.6806	-0.1619	-2.0419
49	N	4.7978	1.9386	0.2801	4.7978	1.9386	0.2801
50	Ru	4.5491	-0.1390	0.0480	4.5491	-0.1390	0.0480
51	H	8.4099	-1.3613	3.1800	8.4099	-1.3613	3.1800
52	H	6.8382	-1.0080	4.5452	6.8382	-1.0080	4.5452
53	H	4.8527	-0.6446	6.0016	4.8527	-0.6446	6.0016
54	H	10.1656	-1.6504	1.4397	10.1656	-1.6504	1.4397
55	H	3.4696	-5.8265	-1.4537	3.4696	-5.8265	-1.4537
56	H	4.7672	-0.4973	-5.9207	4.7672	-0.4973	-5.9207
57	C	-2.4125	1.7039	-0.6510	-2.4125	1.7039	-0.6510
58	C	-2.9314	1.5314	-1.9421	-2.9314	1.5314	-1.9421
59	C	-3.1088	1.2692	0.4867	-3.1088	1.2692	0.4867
60	C	-4.1736	0.8961	-2.0981	-4.1736	0.8961	-2.0981
61	H	-2.3766	1.8846	-2.8058	-2.3766	1.8846	-2.8058
62	C	-4.3532	0.6408	0.3321	-4.3532	0.6408	0.3321
63	H	-2.6879	1.4264	1.4752	-2.6879	1.4264	1.4752
64	C	-4.8860	0.4495	-0.9620	-4.8860	0.4495	-0.9620
65	H	-4.5835	0.7512	-3.0943	-4.5835	0.7512	-3.0943
66	H	-4.9062	0.3010	1.2001	-4.9062	0.3010	1.2001
67	H	4.7707	5.8330	0.6884	4.7707	5.8330	0.6884
68	C	2.2718	4.7151	0.2256	2.2718	4.7151	0.2256

69	C	1.1230	3.9919	-0.0093	1.1230	3.9919	-0.0093
70	H	2.2300	5.7955	0.3301	2.2300	5.7955	0.3301
71	H	0.1619	4.4863	-0.0936	0.1619	4.4863	-0.0936
72	C	0.0176	1.7462	-0.3817	0.0176	1.7462	-0.3817
73	O	-1.1841	2.4209	-0.4861	-1.1841	2.4209	-0.4861
74	C	-8.0791	-0.5298	0.2142	-8.0791	-0.5298	0.2142
75	C	-8.7038	0.7162	-0.1079	-8.7038	0.7162	-0.1079
76	C	-8.8748	-1.4682	0.9384	-8.8748	-1.4682	0.9384
77	C	-10.0488	0.9734	0.1539	-10.0488	0.9734	0.1539
78	C	-10.2058	-1.2110	1.2428	-10.2058	-1.2110	1.2428
79	H	-8.4422	-2.4080	1.2530	-8.4422	-2.4080	1.2530
80	C	-10.8010	-0.0004	0.8250	-10.8010	-0.0004	0.8250
81	H	-10.4977	1.9198	-0.1255	-10.4977	1.9198	-0.1255
82	H	-10.7945	-1.9416	1.7851	10.7945	-1.9416	1.7851
83	N	-7.9440	1.8592	-0.6541	-7.9440	1.8592	-0.6541
84	N	-12.1995	0.2576	1.1112	-12.1995	0.2576	1.1112
85	O	-7.0010	2.3461	0.0577	-7.0010	2.3461	0.0577
86	O	-8.3341	2.3746	-1.7590	-8.3341	2.3746	-1.7590
87	O	-12.8745	-0.6335	1.7463	-12.8745	-0.6335	1.7463
88	O	-12.7193	1.3677	0.7201	-12.7193	1.3677	0.7201
89	N	-6.1567	-0.1417	-1.1528	-6.1567	-0.1417	-1.1528
90	H	-6.4346	-0.3685	-2.1076	-6.4346	-0.3685	-2.1076
91	N	-6.7705	-0.8406	-0.1442	-6.7705	-0.8406	-0.1442
92	S	-6.1741	-2.7740	-0.0140	-6.1741	-2.7740	-0.0140
93	O	-7.3313	-3.7076	-0.7054	-7.3313	-3.7076	-0.7054
94	O	-5.9929	-3.0294	1.5921	-5.9929	-3.0294	1.5921
95	O	-4.7953	-2.6758	-0.8761	-4.7953	-2.6758	-0.8761

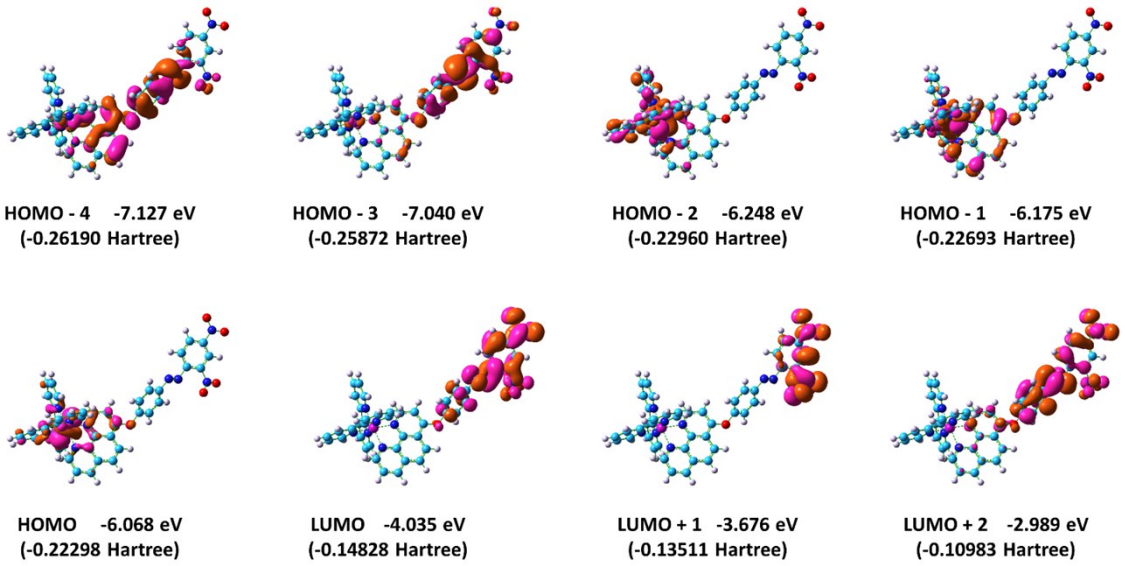

Fig. S14. Representative frontier molecular orbital distributions of **Ru-azo** and their corresponding energies at ground state (S_0) optimized geometries (isodensity contour = 0.02 a.u.).

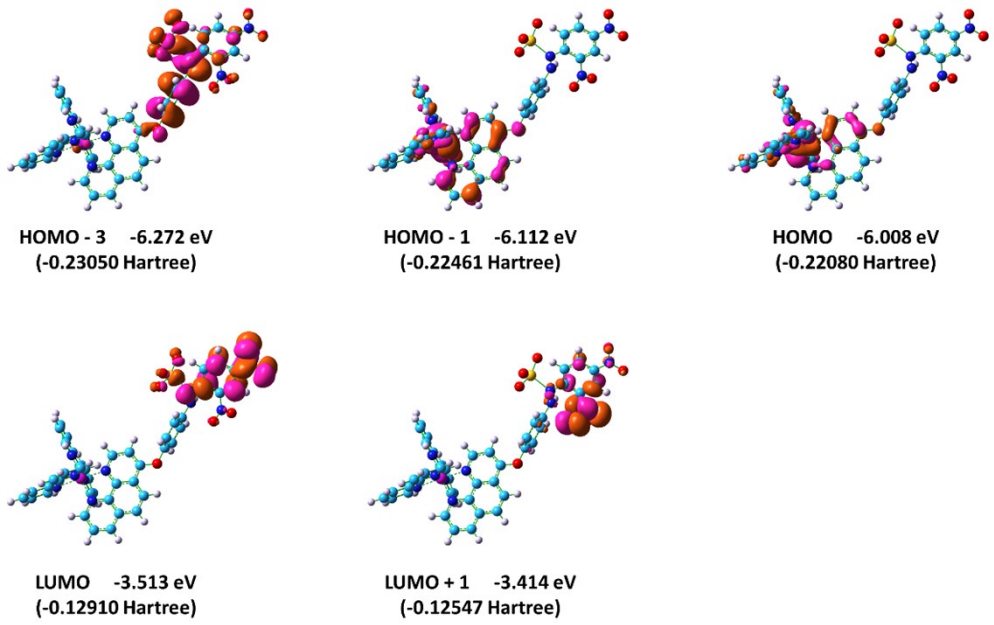

Fig. S15. Representative frontier molecular orbital distributions of **Ru-SO3** and their corresponding energies at ground state (S_0) optimized geometries (isodensity contour = 0.02 a.u.).

Table S3. Absorptions of **Ru-azo** and **Ru-SO3** in aqueous solution from the calculation conducted by TDDFT//B3LYP//6-311+G(d, p), based on the optimized molecular geometries in the ground state.

Complexes	State	Energy (eV) [a]	Wavelength (nm)	*f* [b]	Composition [c]	Contribution [d] (%)	Assignment [e]
Ru-azo	S_1	1.8115	684.42	0.0209	HOMO→LUMO	99.07	ET
	S_2	1.9156	647.24	0.0485	HOMO-1→LUMO	98.92	ET
	S_3	1.9979	620.56	0.0010	HOMO-2→LUMO	99.41	ET
	S_4	2.0939	592.13	0.0504	HOMO-4→LUMO	20.12	ET, IL'CT
					HOMO-3→LUMO	63.04	ET, IL'CT
	S_5	2.1964	564.50	0.0001	HOMO→LUMO+1	99.23	ET
Ru-SO3	S_1	2.1352	580.67	0.0229	HOMO-3→LUMO+1	87.07	IL'CT
	S_2	2.3061	537.64	0.0015	HOMO→LUMO	97.29	ET
	S_3	2.3514	527.28	0.0637	HOMO-3→LUMO	88.42	IL'CT
					HOMO→LUMO+1	10.26	ET
	S_4	2.3067	525.20	0.0078	HOMO→LUMO+1	87.41	ET
	S_5	2.4122	513.99	0.0024	HOMO-1→LUMO	90.90	ET, IL'CT

[a]Only the selected low-lying excited states are presented. [b]Oscillator strength. [c]Only the main configurations are presented. [d]Contributions over 10% are presented. IL'CT: intraligand charge transfer; ET: electron transfer (L: bpy; L': azo-phen or SO3-phen).

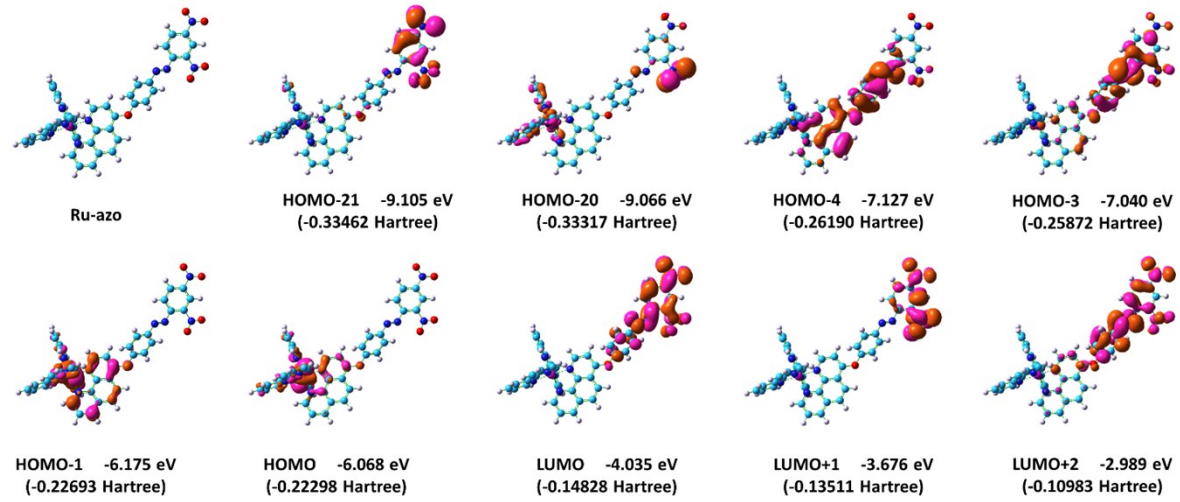

Fig. S16. Representative frontier molecular orbital distributions of **Ru-azo** and their corresponding energies at excited state (T_1) optimized geometries (isodensity contour = 0.02 a.u.).

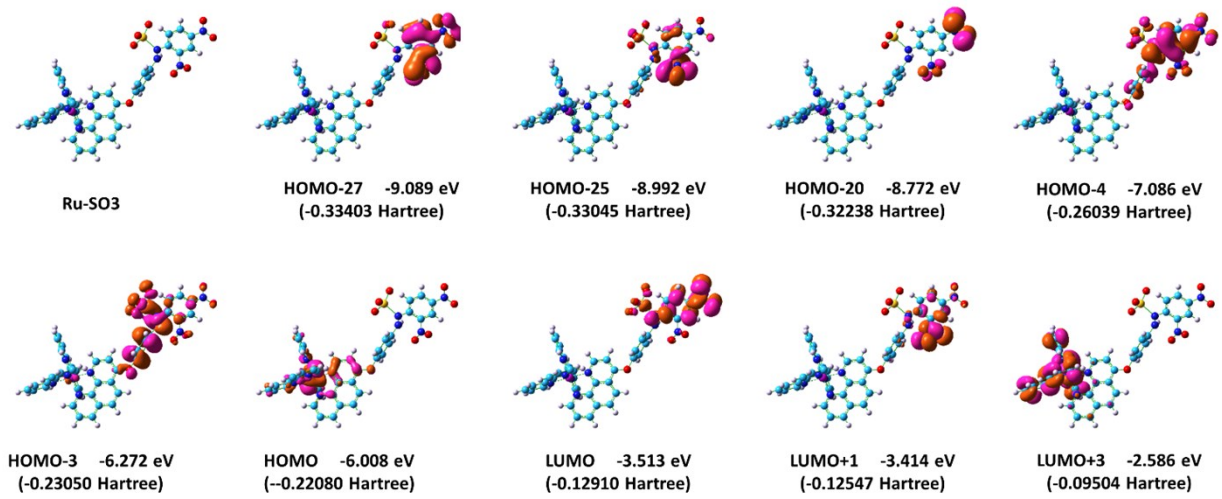

Fig. S17. Representative frontier molecular orbital distributions of **Ru-SO3** and their corresponding energies at excited state (T_1) optimized geometries (isodensity contour = 0.02 a.u.).

4. Supplementary phosphorescence and TGL detection results

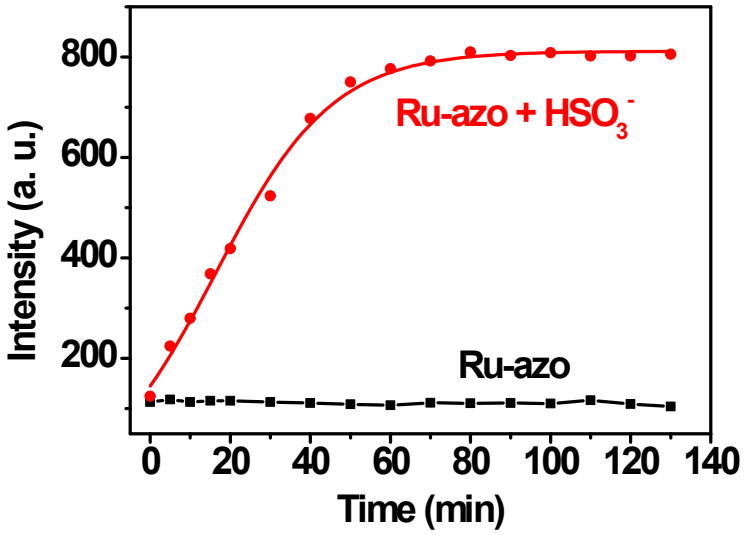

Fig. S18. Time-dependent phosphorescence response (λ_{ex} = 466 nm, λ_{em} = 635 nm) of **Ru-azo** (10 μM) to the addition of bisulfite (500 μM).

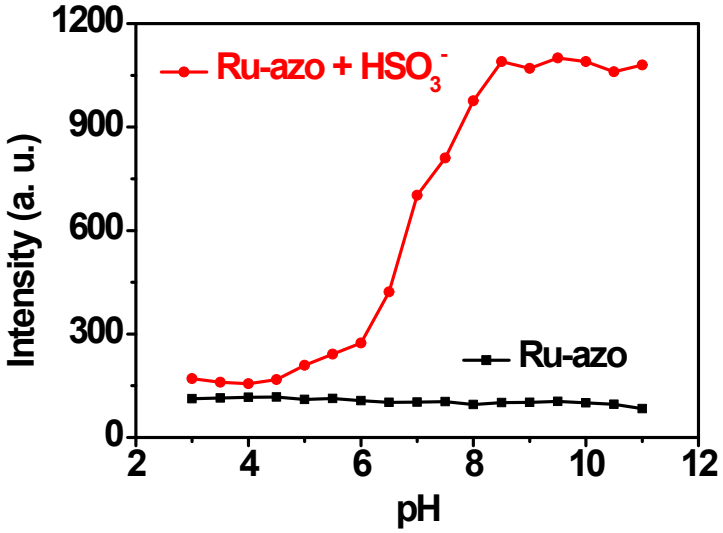

Fig. S19. Effects of pH on the phosphorescence intensity (λ_{ex} = 466 nm, λ_{em} = 635 nm) of **Ru-azo** (10 μM) in the absence and presence of bisulfite (500 μM).

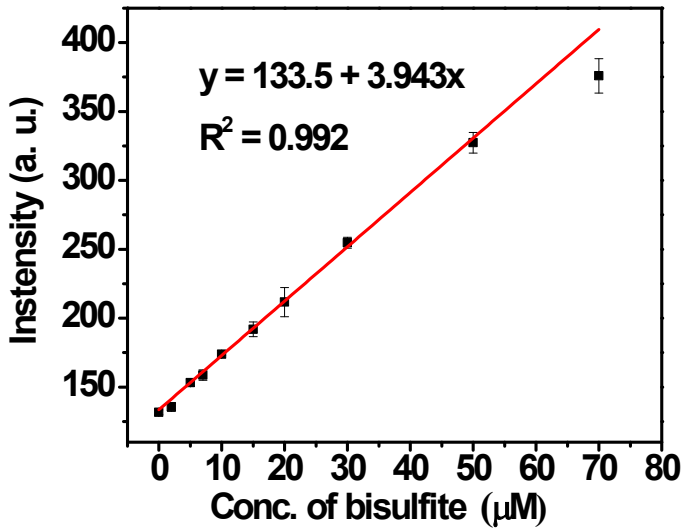

Fig. S20. Correlation between the phosphorescence intensity and bisulfite concentration after **Ru-azo** (10 μM) was reacted with different concentrations of bisulfite in 25 mM PBS buffer of pH 7.4.

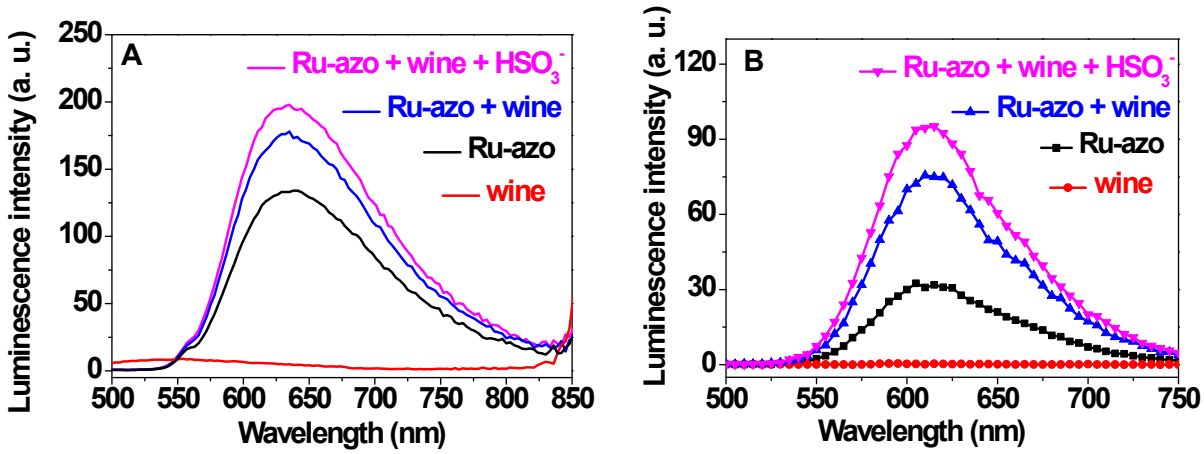

Fig. S21. Phosphorescence (A, 0 ns delay) and TGL (B, 100 ns delay) emission spectra (λ_{ex} = 450 nm) of **Ru-azo** (10 μM), 50-fold diluted wine, and **Ru-azo** (10 μM) in 50-fold diluted wine before and after addition of bisulfite (5.0 μM).

5. Reference

1. Klosterman, J. K.; Linden, A.; Siegel, J. S., Synthesis of aryl-substituted 2-pyridyl-1,10-phenanthrolines; a series of oriented terpyridine analogues. *Organic & Biomolecular Chemistry* **2008,** *6* (15), 2755-2764.

2. Liu, C.; Zhang, R.; Zhang, W.; Liu, J.; Wang, Y.-L.; Du, Z.; Song, B.; Xu, Z. P.; Yuan, J., "Dual-Key-and-

Lock" Ruthenium Complex Probe for Lysosomal Formaldehyde in Cancer Cells and Tumors. *Journal of the American Chemical Society* **2019,** *141* (21), 8462-8472.

3. Sullivan, B. P.; Salmon, D. J.; Meyer, T. J., Mixed phosphine 2,2'-bipyridine complexes of ruthenium. *Inorganic Chemistry* **1978,** *17* (12), 3334-3341.

4. Frisch, M. J.; Trucks, G. W.; Schlegel, H. B.; Scuseria, G. E.; Robb, M. A.; Cheeseman, J. R.; Scalmani, G.; Barone, V.; Mennucci, B.; Petersson, G. A.; Nakatsuji, H.; Caricato, M.; Li, X.; Hratchian, H. P.; Izmaylov, A. F.; Bloino, J.; Zheng, G.; Sonnenberg, J. L.; Hada, M.; Ehara, M.; Toyota, K.; Fukuda, R.; Hasegawa, J.; Ishida, M.; Nakajima, T.; Honda, Y.; Kitao, O.; Nakai, H.; Vreven, T.; Montgomery Jr., J. A.; Peralta, J. E.; Ogliaro, F.; Bearpark, M. J.; Heyd, J.; Brothers, E. N.; Kudin, K. N.; Staroverov, V. N.; Kobayashi, R.; Normand, J.; Raghavachari, K.; Rendell, A. P.; Burant, J. C.; Iyengar, S. S.; Tomasi, J.; Cossi, M.; Rega, N.; Millam, N. J.; Klene, M.; Knox, J. E.; Cross, J. B.; Bakken, V.; Adamo, C.; Jaramillo, J.; Gomperts, R.; Stratmann, R. E.; Yazyev, O.; Austin, A. J.; Cammi, R.; Pomelli, C.; Ochterski, J. W.; Martin, R. L.; Morokuma, K.; Zakrzewski, V. G.; Voth, G. A.; Salvador, P.; Dannenberg, J. J.; Dapprich, S.; Daniels, A. D.; Farkas, Ö.; Foresman, J. B.; Ortiz, J. V.; Cioslowski, J.; Fox, D. J. *Gaussian 09*, Gaussian, Inc.: Wallingford, CT, USA, 2009.

5. Scalmani, G.; Frisch, M. J.; Mennucci, B.; Tomasi, J.; Cammi, R.; Barone, V., Geometries and properties of excited states in the gas phase and in solution: Theory and application of a time-dependent density functional theory polarizable continuum model. *The Journal of Chemical Physics* **2006,** *124* (9), 094107.

6. Lee, C.; Yang, W.; Parr, R. G., Development of the Colle-Salvetti correlation-energy formula into a functional of the electron density. *Physical Review B* **1988,** *37* (2), 785-789.

7. Wang, J.; Bai, F.-Q.; Xia, B.-H.; Zhang, H.-X., Efficient Blue-Emitting Ir(III) Complexes with Phosphine Carbanion-Based Ancillary Ligand: A DFT Study. *The Journal of Physical Chemistry A* **2011,** *115* (42), 11689-11695.

8. Ji, S.; Guo, H.; Wu, W.; Wu, W.; Zhao, J., Ruthenium(II) Polyimine–Coumarin Dyad with Non-emissive 3IL Excited State as Sensitizer for Triplet–Triplet Annihilation Based Upconversion. *Angewandte Chemie International Edition* **2011,** *50* (36), 8283-8286.

9. Cossi, M.; Barone, V., Time-dependent density functional theory for molecules in liquid solutions. *The Journal of Chemical Physics* **2001,** *115* (10), 4708-4717.